Journal of Materials Chemistry C

RSC Publishing

PAPER

View Article Online
View Journal | View Issue

Cite this: J. Mater. Chem. C, 2013, 1, 5976

Synthesis of $L1_0$ ferromagnetic CoPt nanopowders using a single-source molecular precursor and water-soluble support†

Matthew S. Wellons,[a] Zheng Gai,[b] Jian Shen,‡[c] James Bentley,§[b] James E. Wittig[d] and Charles M. Lukehart*[a]

Received 26th June 2013
Accepted 5th August 2013

DOI: 10.1039/c3tc31232a

www.rsc.org/MaterialsC

Reductive decomposition of $CoPt(CO)_4$(dppe)Me/NaCl composite powder (2 : 98 CoPt precursor : NaCl mass ratio) at 650 °C under getter gas (9 : 1 N_2/H_2) gives black CoPt/NaCl nanocomposites with minimal CoPt nanoparticle coalescence. Aqueous dissolution of the NaCl support permits isolation of ferromagnetic $L1_0$ CoPt nanoparticles of *ca.* 11 nm average diameter as free-flowing black powders. As-prepared CoPt nanopowders exhibit moderate coercivity (4.0 kOe) at 300 K and high coercivity (26.0 kOe) at 5 K consistent with formation of polydisperse $L1_0$ CoPt nanoparticles having high purity and high crystallinity. Co_1Pt_1 nanoparticles are formed with good control of alloy stoichiometry using a single-source precursor by a convenient, scalable single-step process.

Introduction

Nanoscale magnetic materials are being explored for high-density data storage applications and for achieving a better fundamental understanding of ferromagnetism on the nanoscale.[1] Binary metal alloys, such as FePt, CoPt, and FePd, exhibit very large uniaxial magnetocrystalline anisotropy constants ($6.6–10 \times 10^{-7}$ erg cm^{-3} for FePt, 4.9×10^{-7} erg cm^{-3} for CoPt, 1.8×10^{-7} erg cm^{-3} for FePd) and high limiting coercivities (116 kOe for FePt, 123 kOe for CoPt, and 33 kOe for FePd) at the nanoscale, and are of particular interest for ultra-high-density data storage applications.[2] Nanoparticles of these compositions are usually described as having either atomically disordered face-centered cubic (fcc) A1-type lattice structures that exhibit small coercivity and soft, superparamagnetic properties or as atomically ordered $L1_0$-type lattice structures exhibiting high coercivity, large magnetic anisotropy, and hard ferromagnetic properties. Nanoparticles formed below *ca.* 300 °C usually have a disordered fcc atomic structure. Phase transition to an ordered $L1_0$ unit cell for CoPt occurs upon thermal treatment between 600 and 850 °C.[3] Annealing at higher temperatures leads to a decrease in observed coercivity due to phase separation.[3] The search for convenient methods of preparing highly ferromagnetic CoPt nanoparticles is of continued interest, because magnetic properties of as-prepared $L1_0$ MPt alloy nanoparticles have yet to approach predicted limiting values.[2] CoPt alloy nanoparticles are also known to function as chemical CO oxidation catalysts[4] and as electrochemical catalysts for CO or methanol oxidation.[5]

CoPt nanoparticles of near 1 : 1 alloy stoichiometry have been prepared *via* hydrogen reduction,[6,7] borohydride reduction,[8–12] polyol reduction,[13–18] sol–gel methods,[19,20] reverse micelle methods,[21,22] galvanic displacement,[23] evaporation methods,[24–27] ion-beam depositom,[28–30] pulse-laser-deposition/ablation/sputtering methods,[31–35] or by bio-inspired or biomimetic methods.[36,37] Common to these methods is use of separate sources of Co and Pt and a two-step process entailing formation of CoPt nanoparticles with subsequent thermal annealing. Ferromagnetic $L1_0$ FePt nanoparticles exhibiting high coercivity have been prepared in earlier work using single-source molecular precursors,[38,39] and this general synthesis strategy is now extended to CoPt nanoparticle formation.

Ferromagnetic 1 : 1 CoPt nanoparticles are formed in a single-step process by reactive decomposition of a known 1 : 1 CoPt heterodinuclear, cluster complex that serves as a stoichiometric source of both metals. Thermal decomposition of $CoPt(CO)_4$(dppe)Me/NaCl powder composites under a reducing atmosphere (H_2/N_2) at 650 °C followed by simple aqueous dissolution of the NaCl support gives free-flowing 1 : 1 CoPt

[a]Department of Chemistry, Vanderbilt University, Nashville, Tennessee 37235, USA. E-mail: chuck.lukehart@vanderbilt.edu; Fax: +1 615 3431234; Tel: +1 615 3222935
[b]Center for Nanophase Materials Sciences, Oak Ridge National Laboratory, Oak Ridge, TN 37831, USA
[c]Material Sciences and Technology Division, Oak Ridge National Laboratory, Oak Ridge, TN 37831, USA
[d]Department of Electrical Engineering and Computer Science, Vanderbilt University, Nashville, Tennessee 37235, USA

† Electronic supplementary information (ESI) available: See experimental procedures for molecular precursor synthesis and for NaCl ball milling. See DOI: 10.1039/c3tc31232a

‡ Present address: Department of Physics, Fudan University, Shanghai 200433, China.
§ Present address: Microscopy and Microanalytical Sciences, PO Box 7103, Oak Ridge, TN 37831, USA.

nanopowders that exhibit moderate room-temperature ferromagnetism ($H_c = 4.0$ kOe at 300 K) and high ferromagnetism at low temperature ($H_c = 26.0$ kOe at 5 K).

Experimental

Reagents and general methods

All manipulations relevant to organometallic precursors were carried out under a nitrogen atmosphere using standard Schlenk techniques. Solvents used in organometallic synthesis were dried over and distilled from appropriate drying agents under N_2. Reagent chemicals, dichloro(1,5-cyclooctadiene) platinum(II), dicobalt octacarbonyl, and diphenylphosphinoethane (dppe), were purchased from Strem Chemicals, Inc.; all other reagents were purchase from Aldrich. The complex, $CoPt(CO)_4$(dppe)Me,[40] was prepared as described in the literature (see ESI†).

Thermal treatments were conducted inside a quartz tube under continuous gas flow using a one-foot Linberg/Blue tube furnace. Sonication was performed in a glass container immersed in a Bransonic 2510R sonifier. Powder X-ray diffraction (XRD) scans were obtained on a Scintag X_1 θ/θ automated powder X-ray diffractometer with a Cu target, a Peltier-cooled solid-state detector, and a zero-background Si(510) sample support. Characterization by TEM was performed at Vanderbilt University with a 200 kV Philips CM20T TEM and at the ORNL SHaRE User Facility with a 200 kV Philips CM200 FEG TEM. Magnetic measurements were performed at Oak Ridge National Laboratory using a SQUID magnetometer. Bulk elemental chemical microanalyses by inductively coupled plasma/optical emission spectrometry (ICP-OES) were performed by Galbraith Laboratories, Knoxville, TN.

Single-step preparation of $L1_0$ CoPt nanoparticles

In a typical preparation, 0.050 g (0.064 mmol) $CoPt(CO)_4$(dppe)Me was dissolved in a minimum amount of CH_2Cl_2 (0.5 mL) under N_2. To achieve a final composite of 2 wt% total metal loading, 0.815 g (13.9 mmol) of ball-milled anhydrous NaCl (see ESI†) was added to the above solution and was allowed to stir for 15 min. Solvent was removed under reduced pressure producing a free-flowing orange powder. The sample was placed in a glazed ceramic boat and was inserted in the center of a tube furnace. The tube volume was purged with N_2 (20 min) and getter gas (1 : 9 $H_2 : N_2$, 20 min), followed by a reductive decomposition at 650 °C under 1 : 9 $H_2 : N_2$ (4 h). The resulting black powder was allowed to cool to room temperature before removal from the furnace and was very responsive to the applied magnetic field of an external magnet. CoPt nanoparticles were isolated by adding this black powder to 5 mL of water followed by mixing, mild sonication, and centrifugation to give a dark precipitate of metal powder. This procedure was repeated two times to ensure complete dissolution of the NaCl support followed by a final acetone (5 mL) wash. The wet metal powder was dried in air to give as-prepared CoPt nanoparticles as a free-flowing black, ferromagnetic powder. Bulk analysis by ICP-OES [element (wt%)]: Co (19.4); Pt (65.6) or $Co_1Pt_{1.02}$.

Results and discussion

Synthesis and characterization of 1 : 1 $L1_0$ CoPt nanopowder

Solvent evaporation from sodium chloride powder wetted by a solution of $CoPt(CO)_4$(dppe)Me gives an orange precursor/NaCl composite powder. Reactive, thermal decomposition of this composite at 650 °C under a flow of getter gas (9 : 1 N_2/H_2) in a tube furnace forms directly CoPt/NaCl nanocomposite as a black powder. Variation of precursor/water-soluble support mass ratio determines the total metal wt% of the final nanocomposite and provides some control over mean particle size. Precursor loadings of 2 wt% total metal affords CoPt nanoparticles of *ca.* 11 nm average diameter. Dissolution of the NaCl support powder by aqueous trituration gives as-prepared $L1_0$-type CoPt nanoparticles as a free-flowing black powder. Bulk elemental analysis reveals a 1 : 1 Co : Pt atomic ratio, consistent with the metal stoichiometry of the precursor.

TEM micrographs of as-prepared CoPt powder at low and high resolution (Fig. 1) reveal single-crystal nanoparticles of irregular shape showing continuous fringe patterns. An interplanar distance of 0.380 nm, measured from a cross-fringe pattern within a single CoPt nanoparticle, corresponds well to the (001) *d*-spacing (0.370 nm) known for bulk $L1_0$ CoPt. A histogram of CoPt nanoparticle sizes (Fig. 1) reveals a log-normal distribution consistent with particle growth *via* a surface-diffusion process[41] having an average CoPt particle diameter of 11 nm ($\sigma = 7$ nm).

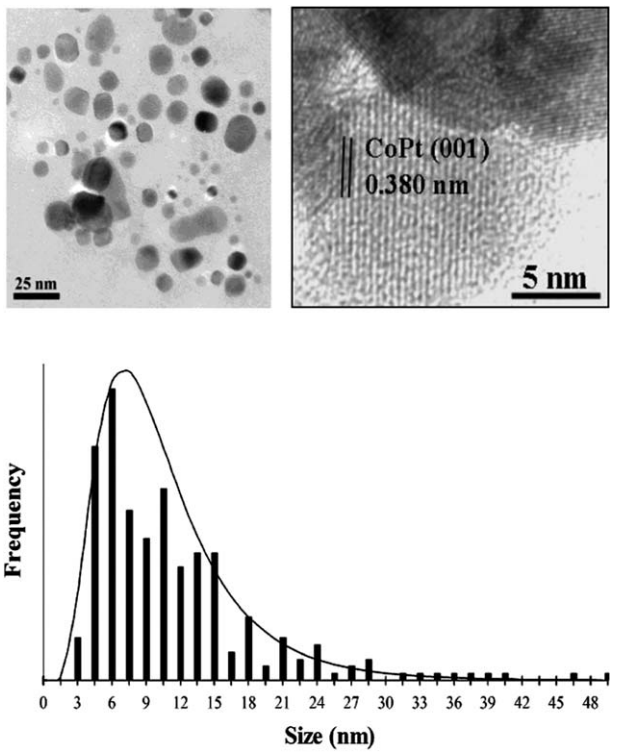

Fig. 1 TEM images of as-prepared $L1_0$ CoPt nanopowder at low (left image) and high (right image) magnification showing (001) lattice fringes expected for $L1_0$ CoPt along with a corresponding particle-size histogram.

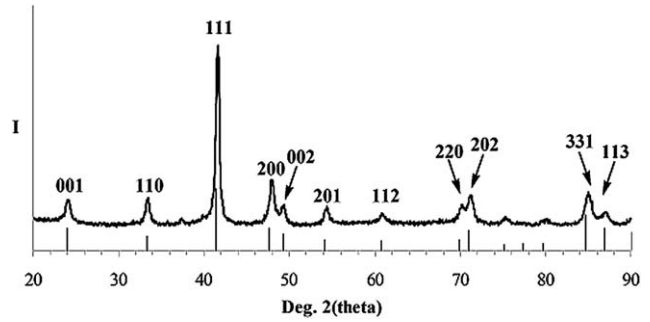

Fig. 2 XRD pattern (Cu K_α radiation) of as-prepared $L1_0$ CoPt nanopowder along with the powder XRD line pattern and assigned peak indices of bulk $L1_0$ CoPt (PDF Card #43-1358).

Successful formation of a highly ordered $L1_0$ lattice for as-prepared CoPt powder is confirmed by powder XRD (Fig. 2). Superlattice peaks expected of a $L1_0$ ordered phase are clearly observed, as evidenced by strong relative intensity of the (001) and (110) diffraction peaks and by splitting of the (200)/(002) pair of reflections. For pure, bulk $L1_0$ CoPt, unit-cell constants are $a = 3.803$ Å and $c = 3.701$ Å giving a c/a ratio of 0.9732.[42] Unit-cell parameters calculated from the experimental XRD pattern (Fig. 2) gives $a = 3.790$ Å and $c = 3.696$ Å and a c/a ratio of 0.9750 confirming formation of highly pure $L1_0$ material.

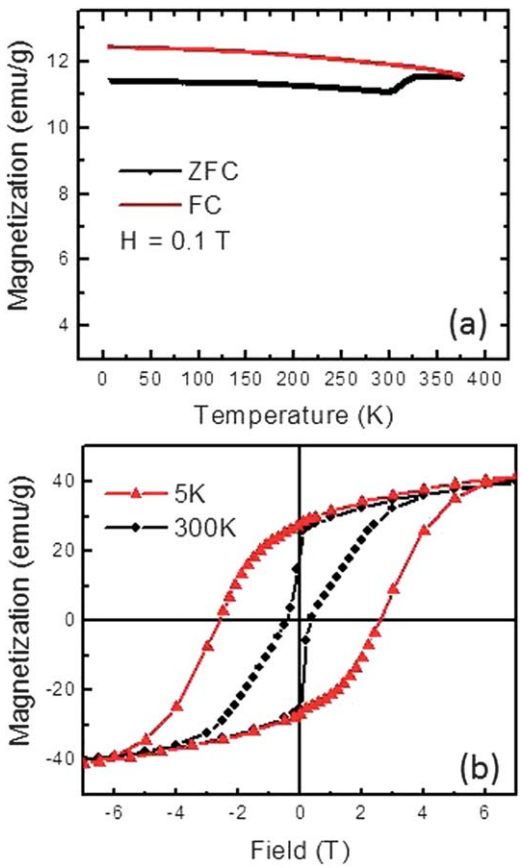

Fig. 3 Temperature and field dependent magnetizations of as-prepared $L1_0$ CoPt nanopowder. (a) ZFC and FC magnetization under 0.1 T field. (b) Magnetic hysteresis loops at 5 K and 300 K.

Scherrer's analysis of experimental $L1_0$ CoPt XRD peak widths gives a volume-weighted average crystallite size of 14 nm. This value compares well with the number-average particle size of 11 nm determined from TEM images and is consistent with only a minor number fraction of particles having diameters $\gg 11$ nm. A diffraction peak centered at 40.50 degrees in two-theta expected for the most intense (111) reflection of a possible $L1_2$ $CoPt_3$ impurity is not observed.

Magnetic properties

Zero field cooled (ZFC) and field cooled (FC) magnetizations at 0.1 T and magnetic hysteresis loops recorded for as-prepared CoPt nanopowder at 5 K and 300 K are shown in Fig. 3. As shown in Fig. 3(a), the superparamagnetic transition is quite broad because of the size distribution of the particles, from really low temperature up to the equipment measurement limit of 380 K. From Fig. 3(b), an observed remanence of $(2/\pi)M_{sat}$ is consistent with a random uniform distribution of magneto-crystalline orientations within the powder specimen.

However, hysteresis loop shapes and coercivity values show strong temperature dependence. At 5 K, a symmetrical ferromagnetic loop shape is observed with a coercivity value of 26.0 kOe. This coercivity is significantly greater than that reported for CoPt nanoparticles prepared by other methods (see Table 1) and is consistent with strong ferromagnetism expected of CoPt nanoparticles having high crystallinity and good control of metal alloy stoichiometry. At 300 K, a highly "pinched" hysteresis loop is observed with a coercivity of 4.0 kOe. While highly

Table 1 CoPt nanoparticulate specimen, processing temperature, nanoparticle average diameters, and measured coercivity values as reported or measured in this work[a]

CoPt sample	Processing T (°C)	CoPt size (nm)	Coercivity, He, (Oe)/temperature	Ref.
CoPt powder	650	11	4000/RT; 26 000/5 K	Herein
CoPt powder	800	18	3202/RT	19
CoPt powder	700	13	3225/RT	20
CoPt powder	800	18	4442/RT	20
CoPt powder	700	18	6000/RT; 9300/5 K	14
CoPt powder	665	$\gg 2$	9000/5 K	10
CoPt powder	650	$\gg 8$	12 000/RT	11
CoPt powder	700	$\gg 4$	7570/RT	16
CoPt powder	550	6	5500/RT	22
CoPt powder	700	>7	630/RT	18
CoPt/SiO_x/Si	700	20	$H_c^{\parallel}$ 8200/Rt; $H_c^{\perp}$ 6636/RT	26
CoPt/SiO_x/Si	750	20	$H_c^{\perp}$ 7400/RT	46
CoPt/SiO_x/Si	750	20	$H_c^{\parallel}$ 7352; $H_c^{\perp}$ 6850/RT	44
CoPt/SiO_x/Si	750	20	$H_c^{\parallel}$ 5558; $H_c^{\perp}$ 4070/RT	47
CoPt/SiO_x/Si	600	5	160/RT; 1900/5 K	15
CoPt/polyimide	650	7	9800/10 K	27, 48
CoPt@PMMA	400	<10	300/300 K; 1665/5 K	12
CoPt@Al_2O_3	1100/700	40 max.	$H_c^{\parallel}$ 4500; $H_c^{\perp}$ 6000/300 K $H_c^{\parallel}$ 9000; $H_c^{\perp}$ 13 000/5 K	29
CoPt@Al_2O_3	700	30	24 200/unspecified	7
CoPt@carbon	800	5.4	1390/RT	6
CoPt@silica	800	30	330/RT	6
CoPt@Ag	550	7–100	1000–17 000/unspecified	49

[a] PMMA = poly(methyl methacrylate); RT = room temperature.

"pinched" CoPt hysteresis loops acquired near room temperature have been ascribed to the presence of a magnetically soft $CoPt_3$ impurity phase,[43] powder XRD data and the high coercivity of this powder at 5 K do not support this interpretation. A more likely explanation of the observed "pinched" hysteresis loop shape is that some number fraction of small CoPt nanoparticles are superparamagnetic near room temperature,[44,45] while those particles bigger than 10 nm still show blocked behavior, giving rise to a combination of superparamagnetic and ferromagnetic effects at 300 K (see the particle-size histogram in Fig. 1). At 5 K, the sample appears wholly ferromagnetic with high coercivity, as expected when thermal energy is insufficient to randomize magnetic dipole oscillations of superparamagnetic particles.

Conclusions

$L1_0$ 1 : 1 CoPt nanoparticles can be prepared in a one-step process by reactive thermal decomposition of $CoPt(CO)_4$(dppe)Me supported on finely ground NaCl powder. Ferromagnetic Co_1Pt_1 powder is harvested by simple aqueous dissolution of the ionic support. Precursor loadings of *ca.* 2 wt% give polydisperse, free-flowing CoPt nanopowders having average diameter of 11 nm and high coercivity (26.0 kOe) at 5 K. This synthesis strategy provides good control of alloy stoichiometry and is both convenient and easily scalable.

Acknowledgements

Financial supported from a Vanderbilt University Discovery Grant is gratefully acknowledged by J.E.W. and C.M.L. Portions of this research were conducted at the Center for Nanophase Materials Sciences and at the SHaRE User Facility of Oak Ridge National Laboratory, both supported by the Division of Scientific User Facilities, Office of Science, U.S. Department of Energy. ORNL is managed by UT-Batelle, LLC, for the U.S. Department of Energy under contract DE-AC05-00OR22725. Work shown in this paper was supported by DOE-BES Grant DE-SC0006877.

Notes and references

1 S. Wirth and S. von Monlnar, *Handbook of Advanced Magnetic Materials*, Springer, New York, 2006, vol. 1, p. 294.
2 P. Entel and M. E. Gruner, *J. Phys.: Condens. Matter*, 2009, **21**, 064228.
3 T. B. Massalski and H. Okamoto, *Binary alloy phase diagrams*, ASM International, Materials Park, Ohio, 2nd edn, 1990.
4 F. Zheng, S. Alayoglu, V. V. Pushkarev, S. K. Beaumont, C. Specht, F. Aksoy, Z. Liu, J. Guo and G. A. Somorjai, *Catal. Today*, 2012, **182**, 54–59.
5 Q.-S. Chen, S.-G. Sun, Z.-Y. Zhou, Y.-X. Chen and S.-B. Deng, *Phys. Chem. Chem. Phys.*, 2008, **10**, 3645–3654.
6 E. Kockrick, F. Schmidt, K. Gedrich, M. Rose, T. A. George, R. Skomski and S. Kaskel, *Chem. Mater.*, 2010, **22**, 1624–1632.
7 Y. Sui, L. Yue, R. Skomski, X. Z. Li, J. Zhou and D. J. Sellmyer, *J. Appl. Phys.*, 2003, **93**, 7571–7573.
8 H. Wan, S. Shi, L. Bai, M. Shamsuzzoha, J. W. Harrell and S. C. Street, *J. Nanosci. Nanotechnol.*, 2010, **10**, 5089–5092.
9 C.-M. Shen, C. Hui, T.-Z. Yang, C.-W. Xiao, S.-T. Chen, H. Ding and H.-J. Gao, *Chin. Phys. Lett.*, 2008, **25**, 1479–1481.
10 H. L. Wang, Y. Zhang, Y. Huang, Q. Zeng and G. C. Hadjipanayis, *J. Magn. Magn. Mater.*, 2004, **272–276**, E1279–E1280.
11 X. Sun, Z. Y. Jia, Y. H. Huang, J. W. Harrel, D. E. Nikles, K. Sun and L. M. Wang, *J. Appl. Phys.*, 2004, **95**, 6747–6749.
12 J. Fang, L. D. Tung, K. L. Stokes, J. He, D. Caruntu, W. L. Zhou and C. J. O'Connor, *J. Appl. Phys.*, 2002, **91**, 8816–8818.
13 B. H. An, J. H. Wu, H. L. Liu, S. P. Ko, J.-S. Ju and Y. K. Kim, *Colloids Surf., A*, 2008, **313–314**, 250–253.
14 V. Tzitzios, D. Niarchos, G. Margariti, J. Fidler and D. Petridis, *Nanotechnology*, 2005, **16**, 287–291.
15 M. Mizuno, Y. Sasaki, M. Inoue, C. N. Chinnasamy, B. Jeyadevan, D. Hasegawa, T. Ogawa, M. Takahashi, K. Tohji, K. Sato, *et al.*, *J. Appl. Phys.*, 2005, **97**, 10J301.
16 C. N. Chinnasamy, B. Jeyadevan, K. Shinoda and K. Tohji, *J. Appl. Phys.*, 2003, **93**, 7583–7585.
17 C. Frommen and H. Rosner, *Mater. Lett.*, 2004, **58**, 123–127.
18 M. Chen and D. E. Nikles, *J. Appl. Phys.*, 2002, **91**, 8477–8479.
19 Y. Liu, Y. Yang, Y. Zhang, Y. Wang, X. Zhang, Y. Jiang, M. Wei, Y. Liu, X. Liu and J. Yang, *Mater. Res. Bull.*, 2013, **48**, 721–724.
20 Y. J. Zhang, Y. T. Yang, Y. Liu, Y. X. Wang, L. L. Yang, M. B. Wei, H. G. Fan, H. J. Zhai, X. Y. Liu, Y. Q. Liu, *et al.*, *J. Phys. D: Appl. Phys.*, 2011, **44**, 295003.
21 U. Wiedwald, L. Han, J. Biskupek, U. Kaiser and P. Ziemann, *Beilstein J. Nanotechnol.*, 2010, **1**, 24–47.
22 A. C. C. Yu, M. Mizuno, Y. Sasaki, H. Kondo and K. Hiraga, *Appl. Phys. Lett.*, 2002, **81**, 3768–3770.
23 X.-W. Zhou, R.-H. Zhang, Y.-X. Jiang and S.-G. Sun, *J. Nanosci. Nanotechnol.*, 2010, **10**, 8265–8270.
24 F. Porrati, E. Begun, M. Winhold, Ch. H. Schwalb, R. Sachser, A. S. Frangakis and M. Huth, *Nanotechnology*, 2012, **23**, 185702.
25 J. Penuelas, C. Andreazza-Vignolle, P. Andreazza, A. Ouerghi and N. Bouet, *Surf. Sci.*, 2008, **602**, 545–551.
26 L. Castaldi, K. Giannakopoulos, A. Travlos, D. Niarchos, S. Boukari and E. Beaurepaire, *Nanotechnology*, 2008, **19**, 085701.
27 J. H. Kim, J. Kim, K. H. Baek, D. H. Im, C. K. Kim and C. S. Yoon, *Colloids Surf., A*, 2007, **301**, 419–424.
28 J. Penuelas, A. Ouerghi, C. Andreazza-Vignolle, J. Gierak, E. Bourhis, P. Andreazza, J. Kiermaier and T. Sauvage, *Nanotechnology*, 2009, **20**, 425304.
29 C. W. White, S. P. Withrow, J. D. Budai, D. K. Thomas, J. M. Williams, A. Meldrum, K. D. Sorge, J. R. Thompson, G. W. Ownby, J. F. Wendelken, *et al.*, *J. Appl. Phys.*, 2005, **98**, 114311.
30 A. Hannour, L. Bardotti, B. Prevel, E. Bernstein, P. Melinon, A. Perez, J. Gierak, E. Bourhis and D. Mailly, *Surf. Sci.*, 2005, **594**, 1–11.
31 F. Tournus, N. Blanc, A. Tamion, M. Hillenkamp and V. Dupuis, *J. Magn. Magn. Mater.*, 2011, **323**, 1868–1872.

32 Z. Y. Pan, R. S. Rawat, J. J. Lin, S. Mahmood, R. V. Ramanujan, P. Lee, S. V. Springham and T. L. Tan, *Appl. Phys. A: Mater. Sci. Process.*, 2010, **101**, 609–613.
33 D. Alloyeau, C. Langlois, C. Ricolleau, Y. Le Bouar and A. Loiseau, *Nanotechnology*, 2007, **18**, 375301.
34 R. K. Rakshit and R. C. Budhani, *J. Phys. D: Appl. Phys.*, 2006, **39**, 1743–1748.
35 Y. Huang, Y. Zhang, G. C. Hadjipanayis, A. Simopoulos and D. Weller, *IEEE Trans. Magn.*, 2002, **38**, 2604–2606.
36 M. T. Klem, D. Willits, D. J. Solis, A. M. Belcher, M. Young and T. Douglas, *Adv. Funct. Mater.*, 2005, **15**, 1489–1494.
37 E. L. Mayes and S. Mann, in *Nanobiotechnology*, ed. C. M. Niemeyer and C. A. Mirkin, 2004, pp. 278–287.
38 R. D. Rutledge, W. H. Morris III, M. S. Wellons, Z. Gai, J. Shen, J. Bently, J. E. Wittig and C. M. Lukehart, *J. Am. Chem. Soc.*, 2006, **128**, 14210–14211.
39 M. S. Wellons, W. H. Morris III, Z. Gai, J. Shen, J. Bentley, J. E. Wittig and C. M. Lukehart, *Chem. Mater.*, 2007, **19**, 2483–2488.
40 A. Fukuoka, S. Fukagawa, M. Hirano, N. Koga and S. Komya, *Organometallics*, 2001, **20**, 2065–2075.
41 C. G. Granqvist and R. A. Buhrman, *J. Catal.*, 1976, **42**, 477–479.
42 Card no. 43–1358, *Powder Diffraction File*, International Center for Diffraction, Newton Square, PA, 1994.
43 V. Karanasos, I. Panagiotopoulos, D. Niarchos, H. Okumura and G. C. Hadjipanayis, *J. Appl. Phys.*, 2000, **88**, 2740–2744.
44 L. Castaldi, K. Giannakopoulos, A. Travlos, D. Narchos, S. Boukari and E. Beaurepaire, *J. Magn. Magn. Mater.*, 2005, **290–291**, 544–546.
45 V. Dupuis, N. Blanc, F. Tournus, A. Tamion, J. Tuaillon-Combes, L. Bardotti and O. Boisron, *IEEE Trans. Magn.*, 2011, **47**, 3358–3361.
46 L. Castaldi, K. Giannakopoulos, A. Travlos, D. Narchos, S. Boukari and E. Beaurepaire, *J. Phys.: Conf. Ser.*, 2005, **10**, 155–158.
47 L. Castaldi, K. Giannakopoulos, A. Travlos and D. Narchos, *Appl. Phys. Lett.*, 2004, **85**, 2854–2856.
48 J. H. Kim, J. Kim, N. Oh, Y.-H. Kim and C. K. Kim, *Appl. Phys. Lett.*, 2007, **90**, 023117.
49 S. Stavroyiannis, I. Panagiotopoulos, D. Niarchos, J. A. Christodoulides, Y. Zhang and G. C. Hadjipanayis, *Appl. Phys. Lett.*, 1998, **73**, 3453–3455.